haematologica
Journal of the Ferrata Storti Foundation

Loss of KDEL function from a calreticulin frameshift mutation drives expression of an immature, mutant calreticulin-dependent form of the thrombopoietin receptor MPL

by Nami Masubuchi, Yinjie Yang, Misa Imai, Yoshihiko Kihara, Soji Morishita, Yoko Edahiro and Norio Komatsu

Received: February 12, 2025.
Accepted: October 24, 2025.

Citation: Nami Masubuchi, Yinjie Yang, Misa Imai, Yoshihiko Kihara, Soji Morishita, Yoko Edahiro and Norio Komatsu. Loss of KDEL function from a calreticulin frameshift mutation drives expression of an immature, mutant calreticulin-dependent form of the thrombopoietin receptor MPL. Haematologica. 2025 Nov 6. doi: 10.3324/haematol.2025.287585 [Epub ahead of print]

Publisher's Disclaimer.
E-publishing ahead of print is increasingly important for the rapid dissemination of science. Haematologica is, therefore, E-publishing PDF files of an early version of manuscripts that have completed a regular peer review and have been accepted for publication.
E-publishing of this PDF file has been approved by the authors.
After having E-published Ahead of Print, manuscripts will then undergo technical and English editing, typesetting, proof correction and be presented for the authors' final approval; the final version of the manuscript will then appear in a regular issue of the journal.
All legal disclaimers that apply to the journal also pertain to this production process.

Loss of KDEL function from a calreticulin frameshift mutation drives expression of an immature, mutant calreticulin-dependent form of the thrombopoietin receptor MPL

Nami Masubuchi[1], Yinjie Yang[1], Misa Imai[1], Yoshihiko Kihara[1], Soji Morishita[1], Yoko Edahiro[1,2], and Norio Komatsu[1,2,3]

[1]Department of Advanced Hematology, Juntendo University Graduate School of Medicine, Tokyo, Japan
[2]Department of Hematology, Juntendo University Graduate School of Medicine, Tokyo, Japan
[3]PharmaEssentia Japan KK, Tokyo, Japan

Corresponding author: Norio Komatsu, Department of Hematology, Juntendo University School of Medicine, 2-1-1, Hongo, Bunkyo-ku, Tokyo, 113-8421 Japan; E-mail: komatsun@juntendo.ac.jp

Running title: Loss of KDEL in mutant CALR and MPL expression

Key words: mutant calreticulin, KDEL, ER retention signal, myeloproliferative neoplasms, MPL

Acknowledgments
We would like to thank other members of the Department of Advanced Hematology and the Department of Hematology for supporting this study. We also acknowledge the Laboratory of Molecular and Biochemical Research, the Laboratory of Morphological Analysis and Imaging, and the Division of Cell Biology in the Research Support Center of the Juntendo University Graduate School of Medicine.

Funding
This work was partially funded by the MEXT-Supported Program for the Strategic

Research Foundation in Private Universities; MEXT's Promotion Plan for the Platform of Human Resource Development for Cancer Project; JSPS KAKENHI Grants #19K08848, #20H03715, #21K16250, #21K08424, #21K08405, #21K08376, and #22K08464.

Authors' contributions

Conceived and designed experiments: NM and NK. Performed experiments: NM, YY, MI, and YK. Analyzed data: NM, YY, MI, SM, and YE. Contributed reagents/materials/analysis tools: NK. Wrote the manuscript: NM and NK.

Competing Interests

N.K has received a salary from PharmaEssentia Japan, where he is a board member; acted as a consultant for Torii Pharmaceutical; received honoraria from Novartis Pharma; received research funding from PharmaEssentia; and is an endowed chair funded by PharmaEssentia Japan.

Data-sharing statement

The data that support the findings of this study are available from the corresponding author upon reasonable request.

Abstract

Mutant calreticulin (CALR) activates the thrombopoietin (TPO) receptor MPL, thereby inducing the development of essential thrombocythemia and primary myelofibrosis. Mutant CALR, due to a frameshift mutation, loses the endoplasmic reticulum (ER) retention signal, the KDEL sequence and is released extracellularly. To examine the significance of the loss of the KDEL sequence in mutant CALR-induced MPL activation, a series of constructs were prepared, including mutant CALR plus KDEL (mutant $CALR^{KDEL}$), mutant CALR plus the Venus tag and KDEL (mutant $CALR^{Venus\text{-}KDEL}$), and wild-type CALR minus KDEL (CALR $WT^{\Delta KDEL}$). UT-7/TPO cells expressing mutant $CALR^{KDEL}$ exhibited autonomous cell growth in the absence of TPO, accompanied by the extracellular secretion of mutant $CALR^{KDEL}$ and subsequent activation of MPL. In contrast, UT-7/TPO cells expressing mutant $CALR^{Venus\text{-}KDEL}$ did not exhibit autonomous cell growth or MPL activation without TPO as well as the reduced extracellular secretion of mutant $CALR^{Venus\text{-}KDEL}$. These results suggest that the loss of KDEL function in mutant CALR is closely linked to MPL activation and the extracellular secretion of mutant CALR. While UT-7/TPO cells expressing CALR $WT^{\Delta KDEL}$ did not exhibit autonomous cell growth, they were responsive to mutant CALR proteins added exogenously, as evidenced by STAT5 activity. Furthermore, CALR $WT^{\Delta KDEL}$ conferred mutant CALR sensitivity to MPL by recognizing the N-glycans of MPL while maintaining it in an immature form, which may bind to mutant CALR. In conclusion, deletion of the ER retention signal KDEL from CALR is a prerequisite for the expression of the immature form of MPL, which can interact with secreted mutant CALR.

Introduction

A somatic mutation in the *calreticulin (CALR)* gene has been identified in the majority of patients with *JAK2*- and *MPL*-unmutated essential thrombocythemia (ET) and primary myelofibrosis, a subset of Philadelphia chromosome-negative myeloproliferative neoplasms (MPNs)[1, 2]. The mutation in the *CALR* gene is a frameshift mutation in the final exon 9, which induces the formation of the mutant CALR-specific carboxyl-terminal (C-terminal) domain[1, 2]. Our research group and others demonstrated that mutant CALR binds to the thrombopoietin (TPO) receptor MPL, resulting in the constitutive activation of downstream signaling molecules of MPL[3-5]. Moreover, our research group showed that mutant CALR forms a homomultimeric complex on its C-terminal domain[6], inducing presumptive structural changes in mutant CALR, that facilitate the amino-terminal domain of mutant CALR to strongly bind to MPL[3]. Wild-type (WT) CALR retains an endoplasmic reticulum (ER) retention signal, the KDEL sequence at the C terminus, and maintains its ER localization by interacting with KDEL receptors in the Golgi apparatus (GA) and transporting them to the ER[7]. However, since mutant CALR lacks the KDEL sequence due to a frameshift mutation, mutant CALR cannot remain in the ER and is secreted from cells that express the mutant protein[8]. Furthermore, mutant CALR has been detected in the plasma of patients with MPNs harboring CALR mutations[9].

Our research group and others demonstrated that mutant CALR and MPL interact on the cell surface, and also that the surface localization of MPL is a prerequisite for mutant CALR-dependent activation[9, 10]. Furthermore, previous studies showed that secreted mutant CALR functions as a ligand, constitutively activating MPL/JAK-STAT signaling in cell lines and patient primary cells[9]. The present study aims to elucidate the importance of the loss of KDEL function in mutant CALR-induced MPL activation.

Methods

Cell culture and proliferation assay

UT-7/TPO cell culture, cell proliferation assay, and transfection were performed as previously described[3]. UT-7/TPO cell lines expressing untagged CALR Del52, Ins5, Del52^{KDEL}, Ins5^{KDEL}, Del52^{Venus}, Ins5^{Venus}, Del52$^{Venus\text{-}KDEL}$, and Ins5$^{Venus\text{-}KDEL}$ were established as previously described[3]. To investigate mutant CALR secreted outside the cell, cells were cultured in Opti-MEM (Gibco, #31985-070) overnight.

Plasmids

To express untagged CALR Del52 and Ins5, plasmids from a previous study were used[10]. In addition, untagged CALR WT and untagged MPL were subcloned into the pcDNA3.1 vector (Life Technologies). Untagged CALR Del52^{KDEL}, CALR Ins5^{KDEL}, CALR Del52^{Venus}, CALR Ins5^{Venus}, CALR Del52$^{Venus\text{-}KDEL}$, CALR Ins5$^{Venus\text{-}KDEL}$, and CALR WT$^{\Delta KDEL}$ were generated through polymerase chain reaction (PCR) mutagenesis (see Supplementary Table 1) and

then subcloned into the pMSCV-IRES-green fluorescence protein vector (Addgene #20672) and pcDNA3.1 vector. A polypeptide linker comprising 10 amino acids (Gly-Gly-Gly-Gly-Ser)$_2$[11] was inserted between the CALR derivatives and Venus. CALR WT$^{\Delta KDEL}$-FLAG-KDEL, untagged CALR WT$^{\Delta KDEL}$ YD/FL, and MPL with an amino acid substitution from asparagine (N) to glutamine (Q) on a potential N-glycosylation site at N117, 178, 298, 358, and the triple mutation of N178/298/358 were created by PCR mutagenesis (see Supplementary Table 1) and subcloned into the pcDNA3.1 vector. C-terminal 6-His-tagged CALR Del52 and Ins5 were created by PCR mutagenesis (see Supplementary Table 1) and subcloned into the pFastBac 1 vector. All constructed plasmids were validated by sequencing.

Confocal microscopy

Immunofluorescence staining was performed as previously described[10, 12]. Fluorescence profiles were analyzed using LAS AF Lite software (Leica).

Immunoblotting analysis

All immunoblot analyses and their quantification were performed as previously described[3, 6, 10]. The following primary antibodies were additionally used in this study: anti-STAT5 (Cell Signaling #94205). Surface CALR was isolated using the Cell Surface Protein Isolation kit (Thermo Fisher Scientific, #89881).

Baculovirus production

Baculoviruses expressing C-terminal 6-His-tagged CALR Del52 and Ins5 were obtained using the Bac-to-Bac Baculovirus Expression System (Gibco #10359016) and TransIT-Insect Transfection Reagent (Mirus #MIR6100) according to the manufacturers' protocols.

Purification of recombinant mutant CALR

Sf9 cells were infected with the P3 baculovirus stock and subsequently cultured for 48 hours. Cells were sonicated in lysis buffer (50 mM Tris [pH 7.4], 0.3 M NaCl, and 0.5 mM PMSF). Cell lysates were then supplemented with imidazole to a final concentration of 20 mM and loaded onto a HisTrap FF column (Cytiva #17531901). Elution was performed with an imidazole using the ÄKTA Pure 25 system (Cytiva, Tokyo, Japan). Purified recombinant mutant CALR was dialyzed in dialysis buffer (50 mM Tris [pH 7.4] and 0.2 M NaCl). The concentration of mutant CALR was determined by Coomassie Brilliant Blue staining, using a BSA standard curve for quantification.

Reporter assay

The reporter assay was performed as previously described[6]. N-glycans ($Glc_1Man_9GlcNAc_2$ (G1M9) and $Man_9GlcNAc_2$ (M9)) purchased from GlyTech, Inc. (Kyoto, Japan).

Statistical Analysis

Data were analyzed using Welch's *t*-test to compare treatment groups with the untreated control. All experiments were independently repeated at least twice or three times, and representative results are shown. Results are presented as the mean ± SD. A p-value < 0.05 was considered statistically significant.

Results

The attachment of the KDEL sequence alone to the C terminus of mutant CALR does not impede its extracellular secretion or the oncogenic activation of MPL

Based on the previous finding showing that mutant CALR activates MPL on the cell surface[9, 10], it was hypothesized that the addition of the KDEL sequence to the C terminus of mutant CALR (mutant CALR^{KDEL}) (Fig. 1a) may result in its retention within the ER, thereby impeding MPL activation. To achieve this, the construct for the expression of mutant CALR^{KDEL} was introduced into the TPO-dependent human megakaryocytic cell line UT-7/TPO[13]. Intracellular fluorescence immunostaining revealed that while mutant CALR localized in the GA (Supplemental Fig. 1a; left panel) as previously reported[9, 10], mutant CALR^{KDEL} accumulated not only in the ER, but also in the GA (Fig. 1b; right panel and Supplemental Fig. 1a; right panel). This result suggests that the function of KDEL was significantly impaired when it directly bound to the C terminus of mutant CALR-specific sequences, resulting in dissociation from the ER and transfer to the cell surface via the GA. To examine the impact of this change in subcellular localization on the tumorgenicity of mutant CALR, the cytokine-independent proliferative capacity of cells was evaluated using a proliferation assay. The results obtained demonstrated that mutant CALR^{KDEL}-expressing cells exhibited TPO-independent cell growth, similar to that observed in cells expressing mutant CALR (Fig. 1c). Furthermore, mutant CALR^{KDEL}-expressing cells showed the cytokine-independent phosphorylation of STAT5, and ERK1/2, downstream signaling molecules of MPL (Fig. 1d). These results indicate that mutant CALR^{KDEL} constitutively activated MPL. The induction of cell growth and the activation of JAK2/STAT5 signaling by exogenous recombinant mutant CALR in Ba/F3 cells artificially expressing both MPL and mutant CALR[9] led to the hypothesis that mutant CALR^{KDEL} may activate MPL after being secreted from cells. Therefore, the culture supernatant was collected and subjected to an immunoblot analysis of secreted proteins, which confirmed that mutant CALR^{KDEL} was secreted from cells into the culture medium (Fig. 1e). These results suggest that some mutant CALR^{KDEL} was released from the ER and was subsequently secreted into the extracellular space, where it activated MPL on the cell surface[10].

The strong inhibition of the extracellular secretion of mutant CALR^{KDEL} diminishes cytokine-independent MPL activation and cell proliferation

Since mutant CALR forms homomultimeric complexes through mutant CALR-specific

sequences at the C terminus[6], we hypothesized that the KDEL sequence in mutant CALR^{KDEL} may not be fully functional as an ER retention signal due to structural complexity. With the aim of creating a construct in which KDEL functions efficiently, the C terminus of mutant CALR was sequentially modified through the addition of the Venus tag and KDEL sequence (mutant CALR$^{Venus\text{-}KDEL}$) (Fig. 2a). The construct was retrovirally transfected into UT-7/TPO cells, and the subcellular localization of mutant CALR$^{Venus\text{-}KDEL}$ to the ER was shown by immunofluorescent staining (Fig. 2b; right panel). In contrast, mutant CALR^{Venus} localized to the GA (Supplemental Fig. 1b; left panel), which mirrored the localization patterns of mutant CALR (Fig. 1b; left panel). Cell proliferation assays were conducted on these cells, and cytokine-independent cell proliferation was observed in mutant CALR^{Venus} without TPO (Fig. 2c). These results were confirmed by the downstream signaling molecules of MPL, STAT5, and ERK1/2 being constitutively phosphorylated in mutant CALR^{Venus} cells in the absence of TPO (Fig. 2d). Therefore, mutant CALR^{Venus}, but not mutant CALR$^{Venus\text{-}KDEL}$, retained its functionality for MPL activation. As shown in Fig. 2e, the secretion of mutant CALR$^{Venus\text{-}KDEL}$ into the extracellular space was markedly reduced compared to that of mutant CALR^{Venus}. On the other hand, mutant CALR$^{Venus\text{-}KDEL}$ was still detectable on the cell surface, as shown in Fig. 2f. These results strongly suggest that the extracellular secretion of mutant CALR was closely linked to mutant CALR-induced MPL activation.

The loss of the KDEL sequence results in the exogenous mutant CALR-induced activation of MPL

To further elucidate the significance of the loss of the KDEL sequence on CALR for autonomous growth and MPL activation, a vector expressing WT CALR without the KDEL sequence (CALR WT$^{\Delta KDEL}$) (Fig. 3a) was generated and introduced into UT-7/TPO cells. CALR WT$^{\Delta KDEL}$-expressing cells lacked autonomous cell growth in the absence of TPO (Fig. 3b). However, the addition of purified recombinant mutant CALR (CALR Del52, CALR Ins5) into these media resulted in concentration-dependent cell proliferation ($p<0.05$) vs. control). Similar results were observed in the mouse leukemia cell line Ba/F3. However, the cells exhibited a sensitive response to the addition of exogenous mutant CALR, presumably due to the enforced overexpression of MPL (Supplementary Fig. 2).

To confirm the activation of MPL by exogenous mutant CALR, a luciferase reporter assay was conducted to assess the transcriptional activity of STAT5, a downstream molecule of MPL signaling, using HEK293T cells. In addition to CALR WT$^{\Delta KDEL}$, C-terminal Flag-tagged WT CALR (CALR WT-FLAG), in which a FLAG tag directly binds to the C-terminal side of the KDEL sequence, was utilized (Fig. 3a). The co-expression of CALR WT-FLAG or CALR WT$^{\Delta KDEL}$ with MPL resulted in the activation of STAT5 by the addition of recombinant mutant CALR proteins, even in the absence of TPO (Fig. 3c). Conversely, the activation of STAT5 was not observed in WT CALR- or CALR WT$^{\Delta KDEL}$-FLAG-KDEL-expressing cells in

which the KDEL sequence was linked to the C-terminal side of the FLAG tag (Fig. 3c) (construct: Fig. 3a). These results suggest that the loss of the KDEL sequence from the C terminus of CALR was imperative for the responsiveness of MPL to exogenous mutant CALR proteins.

The loss of the KDEL sequence in CALR results in the retention of MPL in its immature state of N-glycans

MPL has four N-glycosylation sites (N117, N178, N298, and N358) in its extracellular domain[14], among which N117 of MPL is essential for activation by mutant CALR[11]. To elucidate the mechanisms by which CALR WT$^{\Delta KDEL}$ causes MPL to be activated by extracellular mutant CALR, mutations defective in glycosylation were introduced into each of the N-type glycosylation motifs (N117Q, N 178Q, N298Q, and N358Q) of MPL. Notably, only the MPL harboring the N117 (N117Q) mutation was not activated by mutant CALR proteins (Fig. 4a). Conversely, the activation of MPL by mutant CALR was observed even when all three N-glycosylation motifs, except for N117, were simultaneously mutated (N178/298/358Q) (Fig. 4b). These results indicate that the N-glycosylation of N117 was a prerequisite for the activation of MPL co-expressing CALR WT$^{\Delta KDEL}$ at the cell surface by extracellular mutant CALR.

We subsequently investigated the mechanisms by which CALR WT$^{\Delta KDEL}$ induced mutant CALR-sensitive MPL. It has been well established that CALR functions as a molecular chaperone by recognizing and binding immature N-glycans attached to secreted proteins and receptors in the ER[15, 16]. To elucidate the role of the N-glycan binding of CALR WT$^{\Delta KDEL}$ in the acquisition of mutant CALR sensitivity in MPL, an expression vector of CALR WT$^{\Delta KDEL}$ was constructed, in which a mutation was introduced at the N-glycan recognition site (CALR WT$^{\Delta KDEL\ YD/FL}$), and a luciferase reporter assay was then performed. The co-expression of CALR WT$^{\Delta KDEL\ YD/FL}$ and MPL resulted in the inability of MPL to undergo activation by mutant CALR (Fig. 4c). These results suggest that CALR WT$^{\Delta KDEL}$ conferred mutant CALR sensitivity to MPL by recognizing and binding to the N-glycans of MPL.

Based on previous findings indicating that the glycosylation of MPL was maintained in an immature state in mutant CALR-expressing cells[11], it is plausible that CALR WT$^{\Delta KDEL}$ interacts with MPL within the ER, thereby maintaining the N- glycans of MPL in an immature state and triggering extracellular mutant CALR-mediated MPL activation at the cell surface. It was hypothesized that monoglucosylated immature N-glycans, such as Glc1Man9GlcNAc2 (G1M9), which CALR preferentially recognizes [17, 18], may suppress MPL activation by mutant CALR at the cell surface. To demonstrate this, a STAT5 reporter assay was conducted to evaluate the activation of MPL by recombinant mutant CALR in HEK293T cells co-expressing CALR WT$^{\Delta KDEL}$ and MPL. The impact of immature N-glycans on MPL activation was evaluated by the addition of G1M9, which strongly binds to CALR, or Man9GlcNAc2 (M9), which shows weak CALR binding[19]. G1M9 inhibited STAT5

activation in a dose-dependent manner, while M9 exhibited a lesser degree of inhibition (Fig. 4d). These results indicate that the interaction between CALR WT$^{\Delta KDEL}$ and MPL via the immature N-glycosylation motif played a pivotal role in MPL activation on the cell surface.

Discussion

The present study investigated the significance of the loss of the KDEL sequence in mutant CALR and obtained the following results: (1) some mutant CALR^{KDEL} is transferred from the ER to the GA, is subsequently secreted into the extracellular space, and thereafter activates MPL on the cell surface (Fig. 1 and reference 10); (2) the enhanced ER retention of the mutant CALR protein, induced by the mutant CALR$^{Venus\text{-}KDEL}$ fusion protein, and the subsequent loss of its secretion into the extracellular space result in the elimination of the function of mutant CALR-dependent MPL activation (Fig. 2); (3) the loss of the KDEL sequence from the C terminus of WT CALR results in the ability of MPL to react with purified and recombinant mutant CALR without inducing autonomous cell proliferation (Fig. 3); (4) the activation of MPL on the cell surface is initiated by the interaction between CALR WTΔKDEL and MPL, which occurs via the immature N-glycosylation motif on MPL (Fig. 4). Based on these results, a novel model for the activation of MPL by mutant CALR is proposed, offering a novel perspective on this activation process (Fig. 5). WT CALR associates with MPL in the ER as a molecular chaperone, and this relationship is dissolved when MPL folding is complete. Following the completion of normal folding, MPL is transported from the ER to the GA. Subsequent to this, following the maturation and transport of MPL to the cell surface, mature MPL functions as a TPO receptor, which is not activated by exogenous mutant CALR (Fig. 5A). The newly presented CALR WT$^{\Delta KDEL}$ recognizes and interacts with the immature N-glycans of MPL in the ER. This interaction subsequently results in the transportation of immature MPL to the cell surface, where it is activated by mutant CALR from outside the cell (Fig. 5B). However, CALR WT$^{\Delta KDEL}$ does not induce autonomous cell growth、presumably because it cannot activate immature MPL. Mutant CALR activates MPL by forming homomeric complexes through interactions involving its mutant-specific C-terminus sequence[6]. In contract, CALR WT$^{\Delta KDEL}$ lacks this C-terminal sequences and is therefore likely to exist as a monomer. Further experimental analysis is required to validate this hypothesis.

Based on results from our group and others, we propose three plausible mechanisms by which mutant CALR activates immature MPL (Fig. 5C). In the first model, the mutant CALR remains associated with immature MPL and is co-transported to the cell surface, where it facilitates MPL activation (Fig. 5C, panel a). In the second model, the mutant CALR binds to immature MPL in the endoplasmic reticulum (ER) and escorts it to the cell surface, where MPL is activated in a TPO-independent manner. Following MPL internalization, mutant

CALR dissociates from MPL and is secreted into the extracellular space. The internalized immature MPL is recycled back to the cell surface, where it can rebind secreted mutant CALR, resulting in sustained MPL activation (Fig. 5C, panel b)[20]. In the third model, mutant CALR dissociates from immature MPL before reaching the cell surface, is secreted into the extracellular space, and subsequently rebinds to immature MPL at the cell surface, thereby inducing its activation (Fig. 5C, panel c). While these models are not mutually exclusive, the findings of this study support the latter two models, demonstrating that extracellular mutant CALR can re-engage immature MPL and trigger its activation.

Based on the results showing that mutant $CALR^{KDEL}$-introduced cells grew autonomously and secreted the mutant $CALR^{KDEL}$ protein extracellularly (Fig. 1e), it was hypothesized that the mutant $CALR^{KDEL}$ protein may be activating MPL on the cell surface. The insertion of a Venus tag between the C-terminal region of mutant CALR and the KDEL sequence resulted in the inhibition of both cytokine-independent cell proliferation (Fig. 2c) and the activation of MPL downstream signal molecules (Fig. 2d). On the other hand, these phenomena were not observed when only a Venus tag was added to the C terminus of mutant CALR, thereby ruling out the inhibitory effects of the Venus tag on mutant CALR-induced autonomous cell growth or MPL activation. In normal cells, the KDEL sequence enters the pocket of the transmembrane KDEL receptor in the GA, and these complexes are transported to the ER[21]. In the case of mutant $CALR^{KDEL}$, a mutant CALR-specific sequence to form homo-multimers located immediately before the KDEL sequence may inhibit the association of the KDEL sequence with the KDEL receptor. Consequently, KDEL may lose its function as an ER retention signal. Another explanation for cytokine-independent cell proliferation in mutant $CALR^{KDEL}$ is that immature MPL cannot remain in the ER. This immature MPL may be transported to the cell surface via a secretory pathway, at which it interacts with mutant CALR and is activated. On the other hand, it is conceivable that the majority of mutant $CALR^{Venus\text{-}KDEL}$ remains in the ER (Fig. 2b), thereby preventing the transport of immature MPL to the cell surface. This hypothesis is strongly supported by results showing that the secretion of mutant $CALR^{Venus\text{-}KDEL}$ was significantly reduced compared to that of mutant $CALR^{Venus}$ (Fig. 2e).

While this study provides novel insights into the mechanisms by which mutant CALR activates MPL using cell-based models, several limitations remain to be addressed. First, we were unable to directly demonstrate that secreted mutant CALR binds to MPL on the cell surface and induces its activation, for example via flow cytometry. Therefore, it remains unclear whether MPL activation occurs through co-transport of the mutant CALR-MPL complex to the cell surface, or through the binding of secreted mutant CALR to immature MPL that has independently reached the cell surface. Second, in cells expressing CALR $WT^{\Delta KDEL}$, the precise mechanism by which immature MPL is transported to the cell surface remains unknown. It is not yet clarified whether CALR $WT^{\Delta KDEL}$ induces immature MPL by competitively interfering with the interaction between endogenous CALR WT and

MPL, or by forming heterodimers with CALR WT, thereby preventing CALR WT from retaining immature MPL in the ER. Furthermore, we did not quantitatively assess or compare the direct interactions between MPL and the different CALR constructs used in this study (mutant $CALR^{KDEL}$, mutant $CALR^{Venus}$, mutant $CALR^{Venus\text{-}KDEL}$, and CALR $WT^{\Delta KDEL}$), which limits our understanding of their binding dynamics and functional relevance. In addition, although our findings elucidate this mechanism in cell-based models, further studies using primary hematopoietic cells or in vivo systems are warranted to validate its physiological relevance. In particular, introducing mutant $CALR^{KDEL}$ into primary murine cells may provide deeper insights into its role in hematopoietic transformation and receptor trafficking in a more physiological context.

In conclusion, the deletion of the KDEL sequence by a frameshift mutation in mutant CALR contributes to the development of mutant CALR-positive MPNs through the expression of mutant CALR-responsive immature MPL on the cell surface.

This study was conducted in full accordance with the ethical guidelines of Japan.

References

1. Klampfl T, Gisslinger H, Harutyunyan AS, et al. Somatic mutations of calreticulin in myeloproliferative neoplasms. N Engl J Med. 2013;369(25):2379-2390.

2. Nangalia J, Massie CE, Baxter EJ, et al. Somatic CALR mutations in myeloproliferative neoplasms with nonmutated JAK2. N Engl J Med. 2013;369(25):2391-2405.

3. Araki M, Yang Y, Masubuchi N, et al. Activation of the thrombopoietin receptor by mutant calreticulin in CALR-mutant myeloproliferative neoplasms. Blood. 2016;127(10):1307-1316.

4. Elf S, Abdelfattah NS, Chen E, et al. Mutant Calreticulin Requires Both Its Mutant C-terminus and the Thrombopoietin Receptor for Oncogenic Transformation. Cancer Discov. 2016;6(4):368-381.

5. Chachoua I, Pecquet C, El-Khoury M, et al. Thrombopoietin receptor activation by myeloproliferative neoplasm associated calreticulin mutants. Blood. 2016;127(10):1325-1335.

6. Araki M, Yang Y, Imai M, et al. Homomultimerization of mutant calreticulin is a prerequisite for MPL binding and activation. Leukemia. 2019;33(1):122-131.

7. Sonnichsen B, Fullekrug J, Nguyen Van P, Diekmann W, Robinson DG, Mieskes G. Retention and retrieval: both mechanisms cooperate to maintain calreticulin in the endoplasmic reticulum. J Cell Sci. 1994;107(Pt 10):2705-2717.

8. Liu P, Zhao L, Loos F, et al. Immunosuppression by Mutated Calreticulin Released from Malignant Cells. Mol Cell. 2020;77(4):748-760e9.

9. Pecquet C, Papadopoulos N, Balligand T, et al. Secreted mutant calreticulins as rogue cytokines in myeloproliferative neoplasms. Blood. 2023;141(8):917-929.

10. Masubuchi N, Araki M, Yang Y, et al. Mutant calreticulin interacts with MPL in the secretion pathway for activation on the cell surface. Leukemia. 2020;34(2):499-509.

11. Pecquet C, Chachoua I, Roy A, et al. Calreticulin mutants as oncogenic rogue chaperones for TpoR and traffic-defective pathogenic TpoR mutants. Blood.

2019;133(25):2669-2681.

12. Sunami Y, Araki M, Hironaka Y, et al. Inhibition of the NAD-dependent protein deacetylase SIRT2 induces granulocytic differentiation in human leukemia cells. PLoS One. 2013;8(2):e57633.

13. Komatsu N, Kunitama M, Yamada M, et al. Establishment and characterization of the thrombopoietin-dependent megakaryocytic cell line, UT-7/TPO. Blood. 1996;87(11):4552-4560.

14. Albu RI, Constantinescu SN. Extracellular domain N-glycosylation controls human thrombopoietin receptor cell surface levels. Front Endocrinol (Lausanne). 2011;2:71.

15. Saito Y, Ihara Y, Leach MR, Cohen-Doyle MF, Williams DB. Calreticulin functions in vitro as a molecular chaperone for both glycosylated and non-glycosylated proteins. EMBO J. 1999;18(23):6718-6729.

16. Michalak M, Corbett EF, Mesaeli N, Nakamura K, Opas M. Calreticulin: one protein, one gene, many functions. Biochem J. 1999;344 Pt 2(Pt 2):281-292.

17. Parodi AJ. Role of N-oligosaccharide endoplasmic reticulum processing reactions in glycoprotein folding and degradation. Biochem J. 2000;348 Pt 1(Pt 1):1-13.

18. Hirano M, Adachi Y, Ito Y, Totani K. Calreticulin discriminates the proximal region at the N-glycosylation site of Glc1Man9GlcNAc2 ligand. Biochem Biophys Res Commun. 2015;466(3):350-355.

19. Patil AR, Thomas CJ, Surolia A. Kinetics and the mechanism of interaction of the endoplasmic reticulum chaperone, calreticulin, with monoglucosylated (Glc1Man9GlcNAc2) substrate. J Biol Chem. 2000;275(32):24348-24356.

20. Cleyrat C, Darehshouri A, Steinkamp MP, et al. Mpl traffics to the cell surface through conventional and unconventional routes. Traffic. 2014;15(9):961-982.

21. Gerondopoulos A, Brauer P, Sobajima T, et al. A signal capture and proofreading mechanism for the KDEL-receptor explains selectivity and dynamic range in ER retrieval. Elife. 2021;10:e68380.

Figure Legends

Figure 1: The attachment of the KDEL sequence to the C terminus does not modulate the oncogenic property of mutant CALR

(a) A schematic representation of CALR derivatives characterized in the subsequent analysis. (b) Confocal fluorescence images of UT-7/TPO vector, CALR Del52, CALR Ins5, CALR Del52^{KDEL}, and CALR Ins5^{KDEL} cells after the immunofluorescence labeling of mutant CALR, Calnexin (ER) and nuclei. Scale bar: 10 μm. The intensity profiles of each fluorescent signal in the merged images (indicated by white arrows) are shown as line graphs using the corresponding colors. Black arrows indicate regions of colocalization between mutant CALR and calnexin signals. (c) Cell proliferation assay in the absence (open circle) or presence (closed circle) of 10 ng/mL TPO for UT-7/TPO vector, CALR Del52, CALR Ins5, CALR Del52^{KDEL}, and CALR Ins5^{KDEL} cells. Absorbance was measured at 450 nm to detect the formazan dye produced by viable cells. The mean value and standard deviation (SD) of three replicates are shown. (d) Immunoblot analysis of extracts prepared from UT-7/TPO vector, CALR Del52, CALR Ins5, CALR Del52^{KDEL}, and CALR Ins5^{KDEL} cells cultured in the presence or absence of 10 ng/mL TPO. The y-axis represents the ratio of phosphorylated STAT5 to total STAT5 (bottom, left graph), and phosphorylated ERK to total ERK (bottom, right graph), respectively. The experiment was repeated on three separate occasions. (e) Immunoblot analysis of secreted mutant CALR in the culture supernatant of UT-7/TPO vector, CALR Del52, CALR Ins5, CALR Del52^{KDEL}, and CALR Ins5^{KDEL} cells.

Figure 2: The attachment of the KDEL sequence to the C terminus following the Venus tag impedes the oncogenic property of mutant CALR

(a) A schematic representation of CALR derivatives characterized in the subsequent analysis. (b) Confocal fluorescence images of UT-7/TPO vector, CALR Del52^{Venus}, CALR Ins5^{Venus}, CALR Del52$^{Venus\text{-}KDEL}$, and CALR Ins5$^{Venus\text{-}KDEL}$ cells after the immunofluorescence labeling of mutant CALR, calnexin (ER), and nuclei. Scale bar: 10 μm. The intensity profiles of each fluorescent signal in the merged images (indicated by white arrows) are shown as line graphs using the corresponding colors. Black arrows indicate regions of colocalization between mutant CALR and either calnexin or GM130 signals. (c) Cell proliferation assay in the absence (open circle) or presence (closed circle) of 10 ng/mL TPO for UT-7/TPO vector, CALR Del52^{Venus}, CALR Ins5^{Venus}, CALR Del52$^{Venus\text{-}KDEL}$, and CALR Ins5$^{Venus\text{-}KDEL}$ cells. Absorbance was measured at 450 nm to detect the formazan dye produced by viable cells, and the mean value ± standard deviation (SD) of three replicates is shown. (d) Immunoblot analysis of extracts prepared from UT-7/TPO vector, CALR Del52^{Venus}, CALR Ins5^{Venus}, CALR Del52$^{Venus\text{-}KDEL}$, and CALR Ins5$^{Venus\text{-}KDEL}$ cells cultured in the presence or absence of 10 ng/mL TPO. The y-axis represents the ratio of phosphorylated STAT5 to total

STAT5 (bottom, left graph), and phosphorylated ERK to total ERK (bottom, right graph), respectively. The experiment was independently repeated three times. (e) Immunoblot analysis of secreted mutant CALR in the culture supernatant of UT-7/TPO vector, CALR Del52^{Venus}, CALR Ins5^{Venus}, CALR Del52$^{Venus\text{-}KDEL}$, and CALR Ins5$^{Venus\text{-}KDEL}$ cells. An asterisk indicates non-specific bands detected in vector cell extracts. Each mutant CALR band intensity was quantified and normalized to that of endogenous CALR WT (set as 1). (f) Immunoblot analysis of CALR on the cell surface for the indicated UT-7/TPO cells cultured in the presence or absence of 10 ng/mL TPO.

Figure 3: The removal of the KDEL sequence from wild-type CALR results in the activation of MPL in response to extracellular mutant CALR

(a) A schematic representation of CALR derivatives characterized in the subsequent analysis. (b) Cell proliferation assay in the absence or presence of the indicated amounts of recombinant mutant CALR for UT-7/TPO vector (open bar) and CALR WT$^{\Delta KDEL}$ (solid bar) cells. Absorbance was measured at 450 nm to detect the formazan dye produced by viable cells after 3 days. Data are presented as the mean ± SD of three replicates. The experiment was independently repeated three times with similar results, and representative data are shown. *p<0.05. (c) STAT5 transcriptional activity assessed by the luciferase reporter assay. HEK293T cells expressing wild-type CALR derivatives and MPL were used. Data are represented as the mean ± SD of three replicates. Statistical significance was made between each treatment groups (mutant CALR or TPO) and the untreated control (−) within each experimental condition. *p<0.05.

Figure 4: The extracellular mutant CALR protein requires immature N-type glycans of MPL for MPL activation in CALR WT$^{\Delta KDEL}$-expressing cells

(a) A comparison of STAT5 transcriptional activity by mutant CALR when a mutation is introduced into one of the four N-type glycosylation modification sites (N117Q, N178Q, N298Q, and N358Q) of MPL. Data are shown as the mean ± SD of three replicates. The experiment was independently performed three times with consistent results, and representative data are presented. Statistical significance was assessed between each treatment group (mutant CALR or TPO) and the untreated control (−) within each condition. *p<0.05. (b) A comparison of the STAT5 transcriptional activity of mutant CALR when a mutation is introduced into N117 of MPL (N117Q) or when mutations are introduced into three sites (N178/298/358Q). Data are presented as the mean ± SD of three replicates. The experiment was independently repeated three times with similar outcomes, and representative data are shown. Statistical significance was determined between each treatment group (mutant CALR or TPO) and the untreated control (−). *p<0.05. (c) A comparison of STAT5 transcriptional activity by mutant CALR when a mutation is introduced into the carbohydrate recognition site of CALR WT$^{\Delta KDEL}$ (WT$^{\Delta KDEL}$

YD/FL). Data are shown as the mean ± SD of three replicates. The experiment was independently conducted twice with reproducible results, and representative data are shown. Statistical comparison was performed between each treatment group (mutant CALR or TPO) and the untreated control (−) within each experimental condition. *p<0.05. (d) STAT5 transcriptional activity is shown when N-glycans (M9 or G1M9) are added with recombinant mutant CALR to cells expressing MPL and CALR WT$^{\Delta KDEL}$. STAT5 transcriptional activity was investigated by adding recombinant mutant CALR proteins to HEK293T cells. Data are shown as the mean ± SD of three replicates and are representative of three independent experiments. Statistical significance was evaluated between each treatment group (CALR Del52 plus M9 or G1M9) and the untreated control (CALR Del52 alone). *p<0.05.

Figure 5: A model for the activation of MPL by mutant CALR

(A) In CALR WT-expressing cells, CALR binds MPL with the ER as a molecular chaperone. Following detachment from CALR, the N-glycans of MPL undergo modifications through a secretory pathway and ultimately do not associate with mutant CALR on the cell surface. (B) In cells expressing CALR WT$^{\Delta KDEL}$, CALR WT$^{\Delta KDEL}$ binds the immature N-glycans of MPL in the ER and subsequently transports immature MPL from the ER. Immature MPL localized on the cell surface can be activated by exogenously added mutant CALR protein. (C) Three plausible mechanisms by which mutant CALR activates immature MPL. In panel a, mutant CALR remains associated with immature MPL and is co-transported to the cell surface, where it facilitates MPL activation. In panel b, mutant CALR binds to immature MPL in the endoplasmic reticulum (ER) and escorts it to the cell surface, where MPL is activated in a TPO-independent manner. Following MPL internalization, mutant CALR dissociates from MPL and is secreted into the extracellular space. The internalized immature MPL is recycled back to the cell surface, where it can rebind secreted mutant CALR, resulting in sustained MPL activation. In panel c, mutant CALR dissociates from immature MPL before reaching the cell surface, is secreted into the extracellular space, and subsequently rebinds to immature MPL at the cell surface, thereby inducing its activation.

Figure 1

Masubuchi et al.

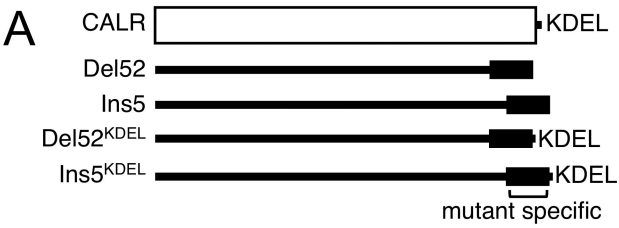

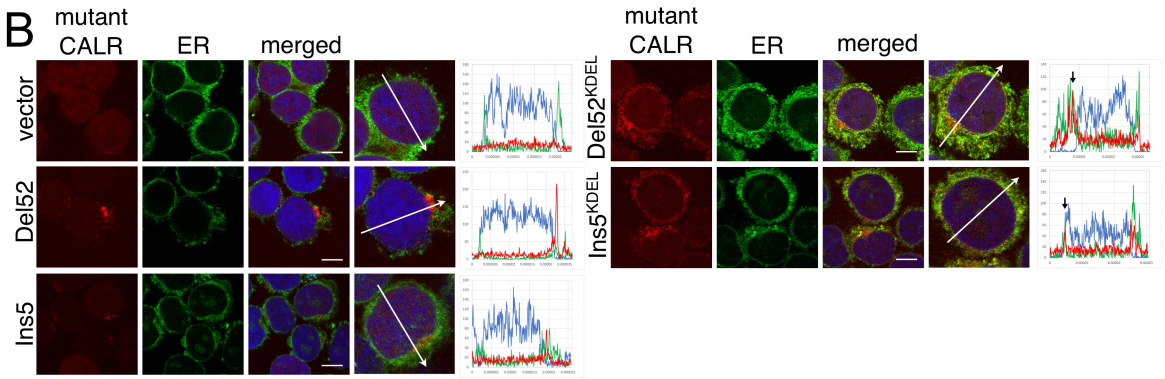

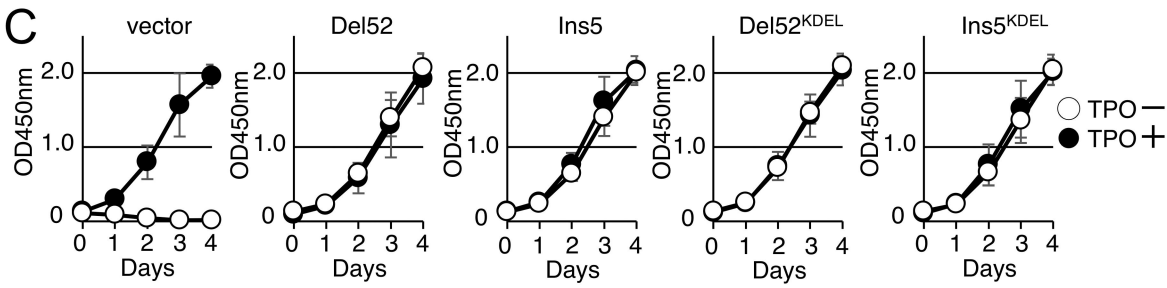

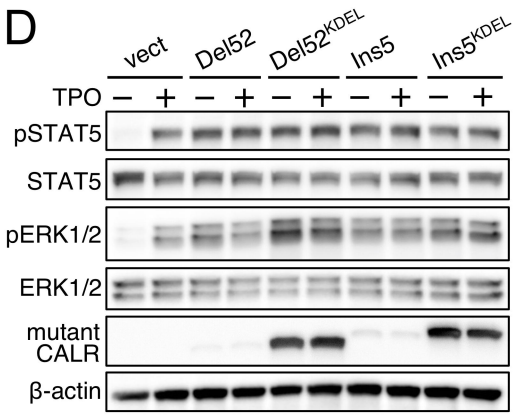

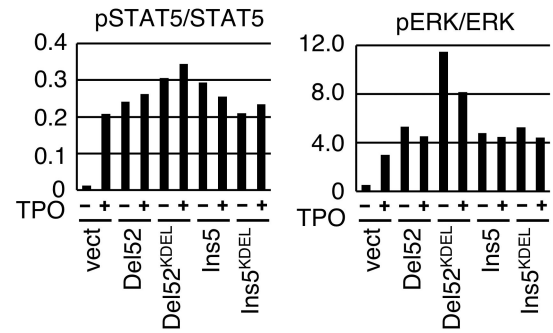

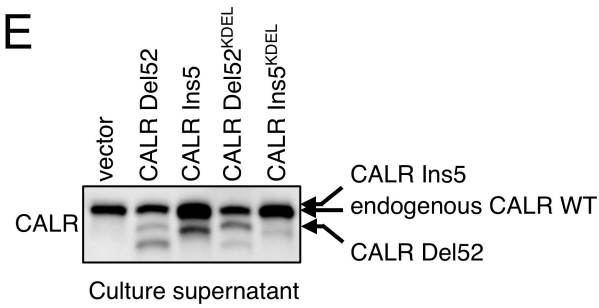

Figure 2

Masubuchi et al.

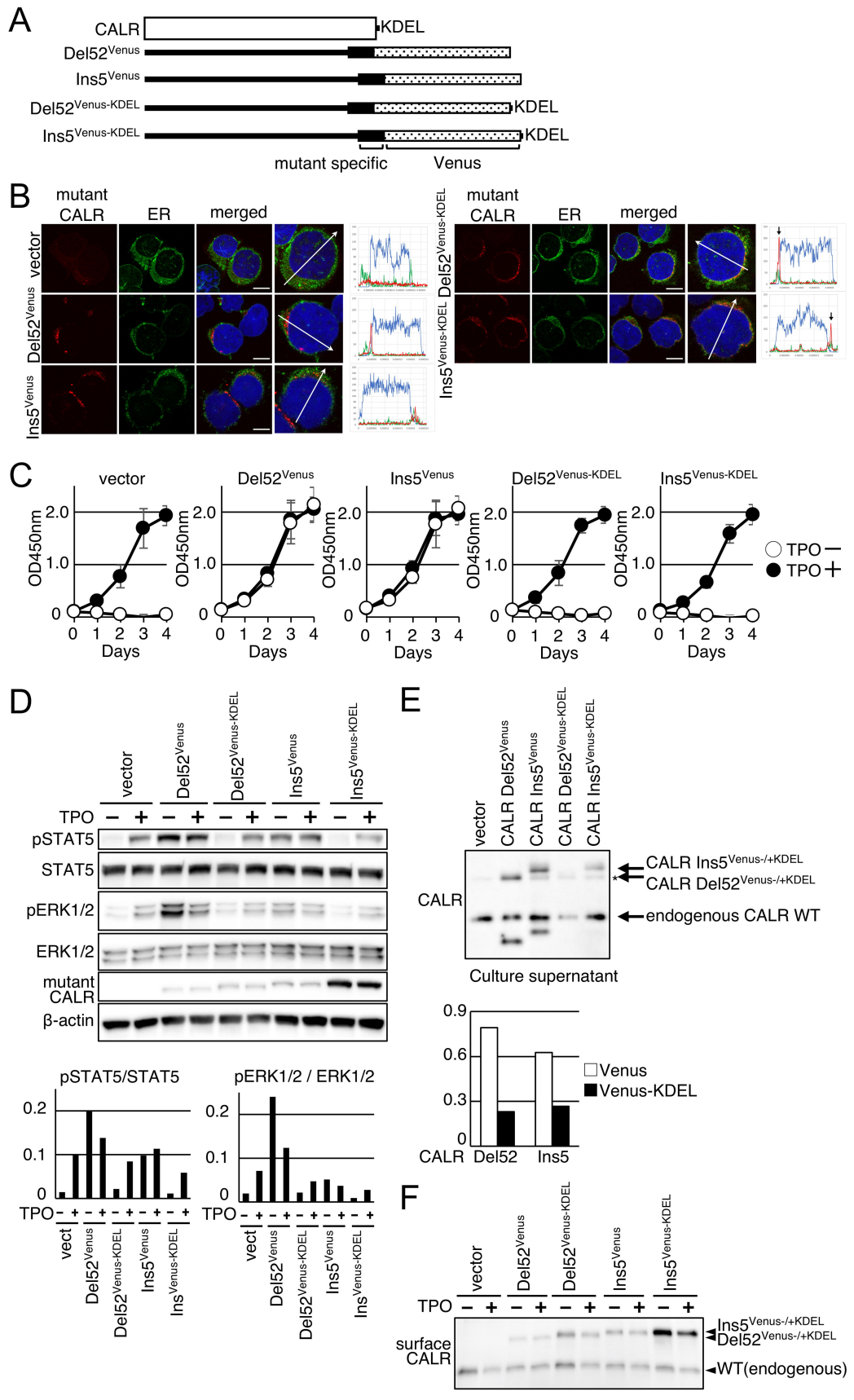

Figure 3

Masubuchi et al.

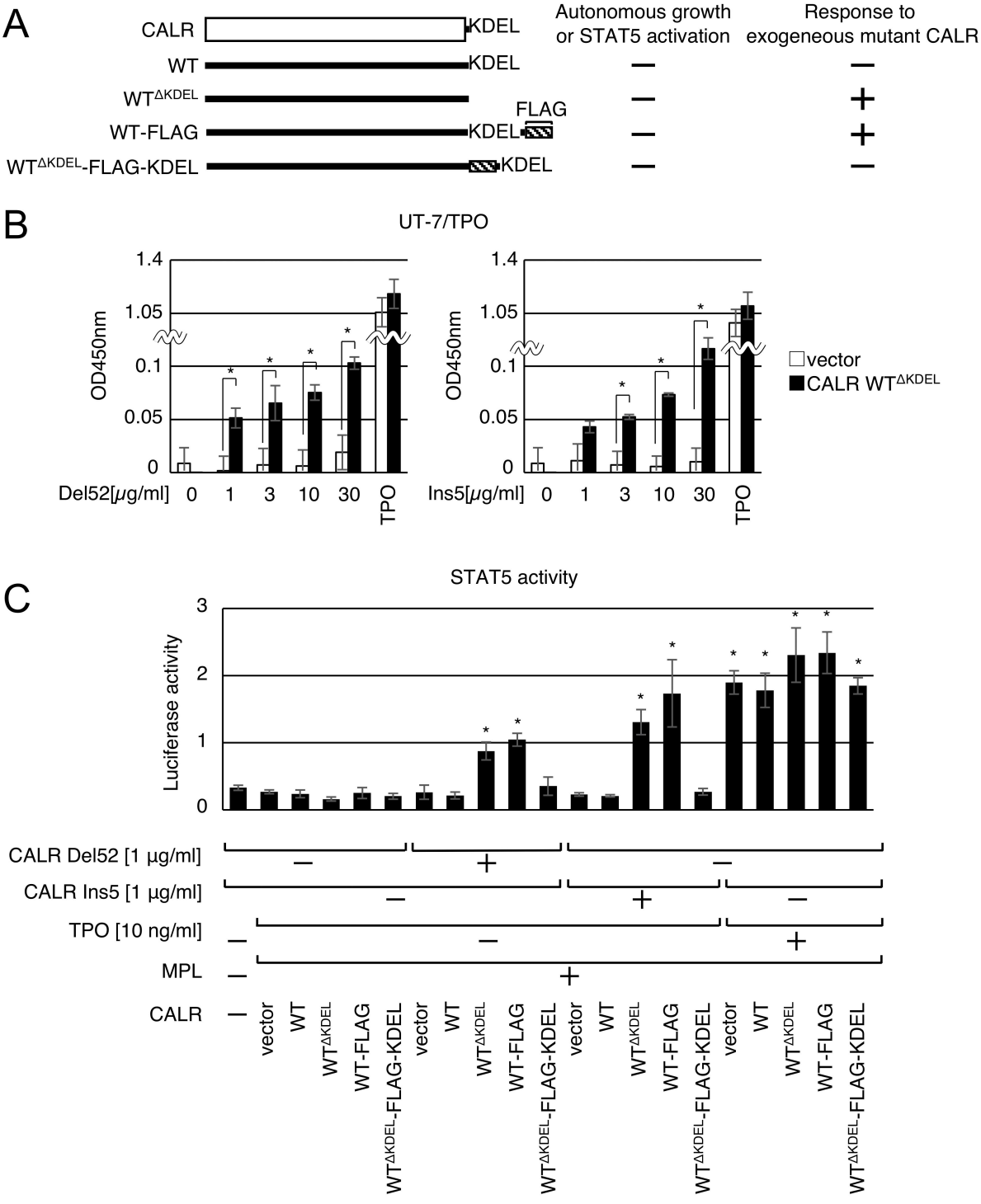

Figure 4

Masubuchi et al.

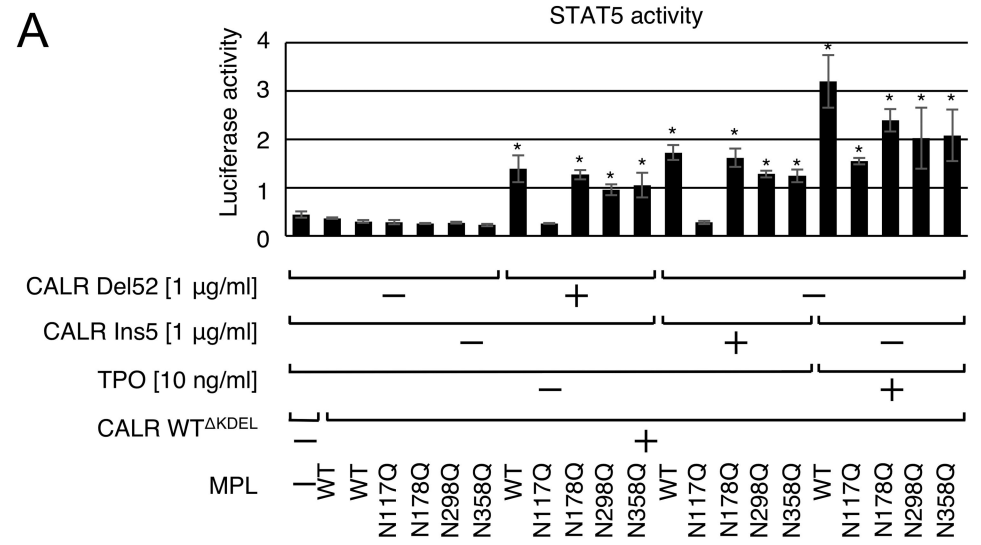

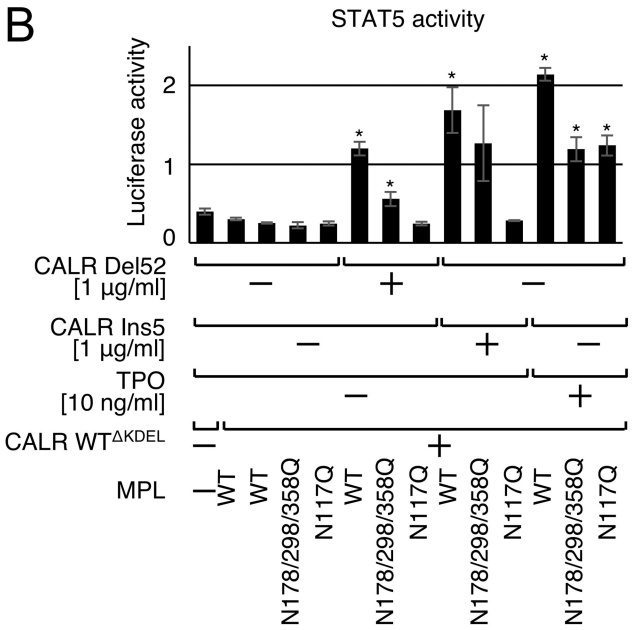

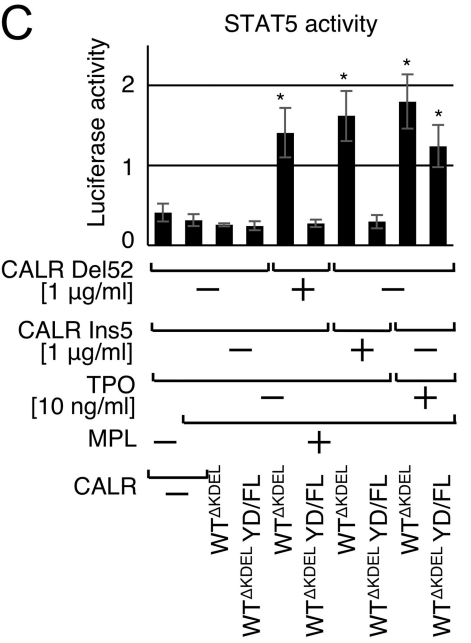

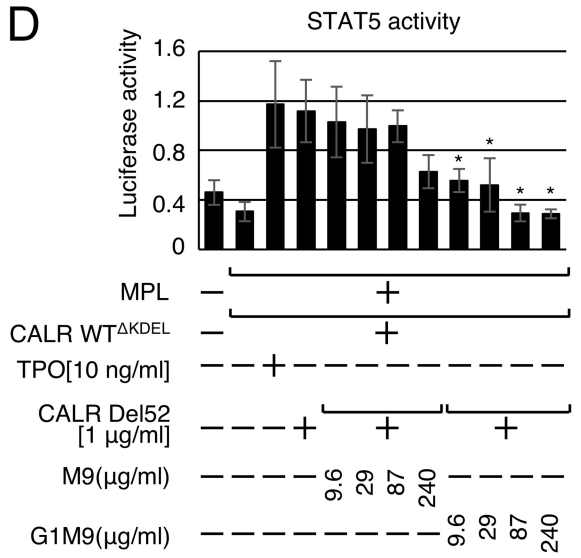

Figure 5

Masubuchi et al.

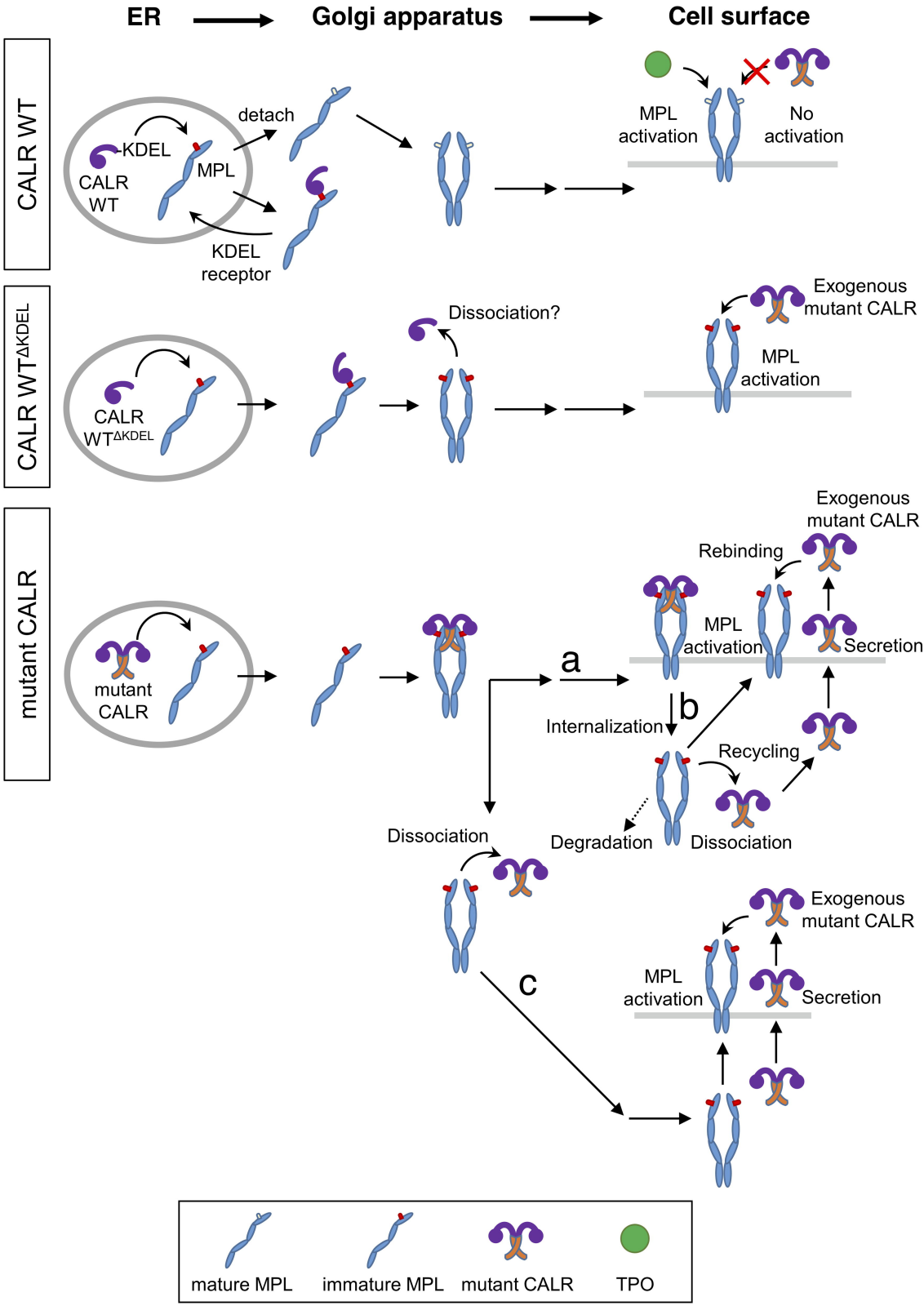

Supplementary Table 1: Primers used for the construction of CALR and MPL derivatives

Primer name	Primer sequence
CALR N-ter_Fw	5'-AAAAGAATTCGCCACCATGCTGCTATCCGTGCCGC-3'
CALRmut+KDEL_Rev	5'-TTTTCTCGAGCTACAGCTCGTCCTTGGCCTCAGTCCAGCCCTGG-3'
CALR N-ter_Fw	5'-AAAAGAATTCGCCACCATGCTGCTATCCGTGCCGCTGCTG-3'
CALRmut+linker Rev(Ron66)	5'-TGATCCTCCACCACCAGATCCACCTCCACC GGCCTCAGTCCAGCCCTGG-3'
Linker+Venus Fw (Ron49)	5'-GGTGGAGGTGGATCTGGTGGTGGAGGATCAATGGTGAGCAAGGGCGAGG-3'
Venus+KDEL Rev(Ron94)	5'-TTTTACCGGTCTACAGCTCGTCCTTCTTGTACAGCTCGTCC-3'
Venus Rev	5'-TTTTACCGGTTTACTTGTACAGCTCGTCCATGCCGAGAG-3'
CMV	5'-CGCAAATGGGCGGTAGGCGTG-3'
CALR WT$^{\Delta KDEL}$_Rev	5'-TTTCTCGAGCTAGGCCTGGCCGGGGACATCTTCC-3'
CMV	5'-CGCAAATGGGCGGTAGGCGTG-3'
CALR WT$^{\Delta KDEL}$+Flag_Rev	5'-TTTATCGTCATCGTCTTTGTAGTCGGCCTGGCCGGGGACATCTTC-3'
Flag+KDEL_Rev	5'-TTGAATTCCTACAGCTCGTCCTTTTTATCGTCATCGTCTTTGTAG-3'
CALR^{Y109F} _Fw	5'-CTGTGGGGGCGGCTTTGTGAAGCTGTTTC-3'
CALR^{Y109F} _Rev	5'-GAAACAGCTTCACAAAGCCGCCCCCACAG -3'
CALR^{D135L} _Fw	5'-CATGTTTGGTCCCCTCATCTGTGGCCCTG-3'
CALR^{D135L} _Rev	5'-CAGGGCCACAGATGAGGGGACCAAACATG-3'
MPL^{N117Q}_Fw	5'-GTGTTCCTACAGCAGACTCGGACTCAGCGAGTCC-3'
MPL^{N117Q}_Rev	5'-CGAGTCTGCTGTAGGAACACATTCTTCACCCAG-3'
MPL^{N178Q}_Fw	5'-GATCCCAAGCAGTCCACTGGTCCCACGGTCATACAG-3'
MPL^{N178Q}_Rev	5'-CCAGTGGACTGCTTGGGATCTCTGGGGCCATAGC-3'
MPL^{N298Q}_Fw	5'-GACCTGAAGCAGGTTACCTGTCAATGGCAGCAAC-3'
MPL^{N298Q}_Rev	5'-CAGGTAACCTGCTTCAGGTCCAAGGTAAAGCATTGC-3'
MPL^{N358Q}_Fw	5'-CAAGTCACGACAGGACAGCATTATTCACATCCTTG-3'
MPL^{N358Q}_Rev	5'-GCTGTCCTGTCGTGACTTGAAGTGGCAGCGAGAG-3'
CALR N-ter_Fw	5'-AAAAGAATTCGCCACCATGCTGCTATCCGTGCCGCTGCTG-3'
CALR mut+6-His_Rev	5'-AAGAATTCTCAGTGATGGTGATGGTGATGGGCCTCAGTCCAGCCCTGG -3'

Supplemental Figure 1 Masubuchi et al.

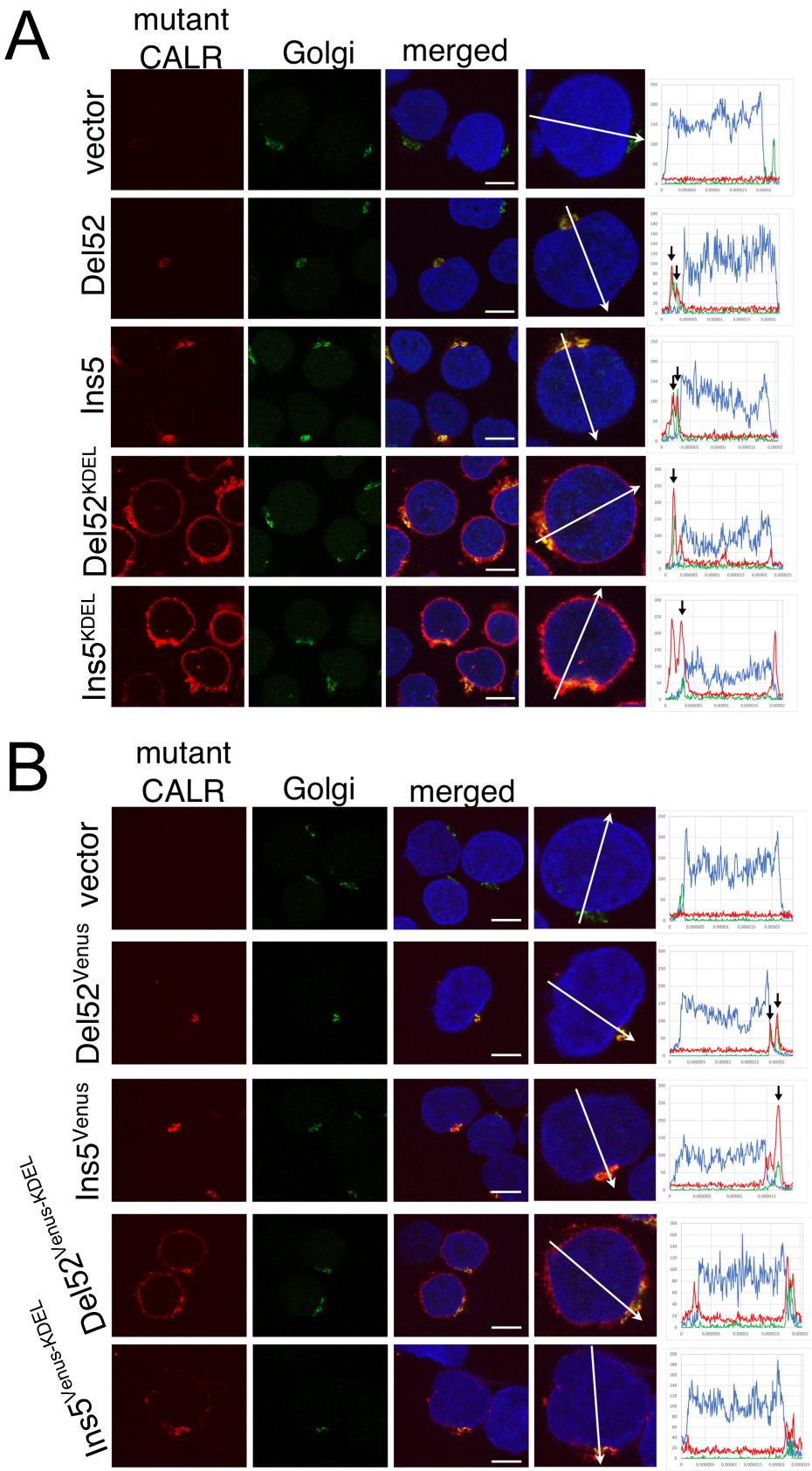

Supplemental Figure 2

Masubuchi et al.

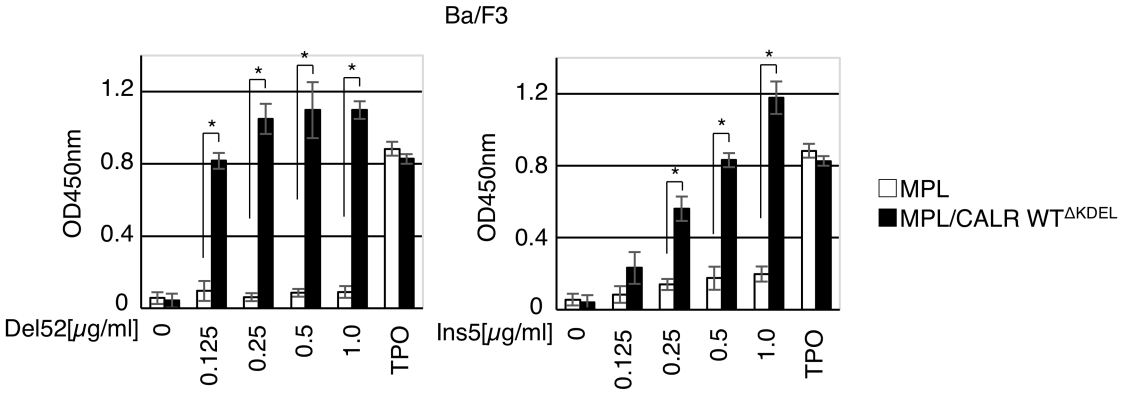

Supplementary Figure 1: (a) Confocal fluorescence images of UT-7/TPO vector, CALR Del52, CALR Ins5, CALR Del52^{KDEL}, and CALR Ins5^{KDEL} cells following immunofluorescence staining for mutant CALR, GM130 (Golgi apparatus), and nuclei. Scale bar: 10 μm. Intensity profiles of each fluorescent signal along the white arrows in the merged images are shown as line graphs using the corresponding colors. Black arrows indicate colocalization between mutant CALR and GM130 signals. (b) Confocal fluorescence images of UT-7/TPO vector, CALR Del52^{Venus}, CALR Ins5^{Venus}, CALR Del52$^{Venus\text{-}KDEL}$, and CALR Ins5$^{Venus\text{-}KDEL}$ cells after immunofluorescence staining for mutant CALR, GM130, and nuclei. Scale bar: 10 μm. Intensity profiles of each fluorescent signal along the white arrows in the merged images are shown as line graphs using the corresponding colors. Black arrows indicate colocalization between mutant CALR and GM130 signals.

Supplementary Figure 2: Cell proliferation assay in the absence or presence of recombinant mutant CALR or TPO in Ba/F3 MPL CALR WT$^{\Delta KDEL}$ cells after three days of culture. Absorbance was measured at 450 nm to detect the formazan dye produced by viable cells after 3 days. Data are presented as the mean ± SD of three replicates. The experiment was independently repeated three times with similar results, and representative data are shown. *p<0.05 was considered statistically significant.

Supplemental Information

Supplemental methods

Plasmids

To express untagged MPL, cDNA was subcloned into the pMSCV-IRES-DsRed FP vector (Addgene #52110).

Cell culture and proliferation assay

Interleukin (IL)-3-dependent Ba/F3 cells were cultured at 37°C in 5% CO_2 in Roswell Park Memorial Institute 1640 medium (Nacalai Tesque, #30264-56) containing 10% fetal bovine serum (Thermo Fisher, #10270-106), 1 ng/ml murine IL-3 (PEPROTECH, #213-13-50UG), 100 U/mL penicillin (Nacalai Tesque, #26239-42), and 100 μg/mL streptomycin (Nacalai Tesque, #32204-92). The cell proliferation assay and transfection were performed as previously described[3].